Achieving Broadband NIR Emission through Multiple Centers of Isolated Cr^{3+} and Cr^{3+}-Cr^{3+} Ion Pairs Resulting from Phase Segregation in $SrLa_2Ga_2O_7$

Xiao-Na Shen,[a] Yu-Guo Yang,[a,*] Hua-Jian Yu,[a] Cheng-Cheng Qiu,[a, c] Wei Zhao,[a] Shuo Sun,[a] Yuan-Yuan Zhang,[a,b] Bing Liu,[a,b] Xian-Shun Lv,[a, c] Rui Zhang,[a,b] Xu-Ping Wang[a, c, ξ]

[a] Advanced Materials Institute, Qilu University of Technology (Shandong Academy of Sciences), Jinan 250014, P.R. China

[b] Shandong Key Laboratory of Silicon Carbide Material, Jinan 250353, P.R. China

[c] Shandong Engineering Research Center of Advanced Optoelectronic Functional Materials and Devices, Jinan 250353, China

[*]Email: yangyuguo@sdas.org

[ξ]Email: wangxp@sdas.org

Experimental section

The X-ray diffraction (XRD) analysis of the phosphor-related materials was performed using a Rigaku SmartLab SE X-ray diffractometer (Japan). The morphology of the samples was examined by scanning electron microscopy (SEM) utilizing a Zeiss Gemini 500. Elemental distribution map was generated via energy dispersive spectroscopy (EDS). The X-ray photoelectron spectroscopy (XPS) analysis of the phosphor was conducted using an ESCALAB XI+ X-ray photoelectron spectrometer. Electron paramagnetic resonance (EPR) measurements were carried out at room temperature using a Bruker EMX PLUS EPR spectrometer. The Raman spectrum of the phosphor was acquired employing a micro-laser confocal Raman spectrometer, specifically the LabRAM HR Evolution. Additionally, the absorption spectrum of the phosphor was recorded with an Agilent Cary 7000 UMS universal spectrophotometer. The optical properties of the phosphor were evaluated using a UV-Vis-NIR fluorescence spectrometer (FLS 1000), including analyses such as excitation spectra (PLE), emission spectra (PL), temperature-dependent photoluminescence spectra, and fluorescence lifetime decay curves.

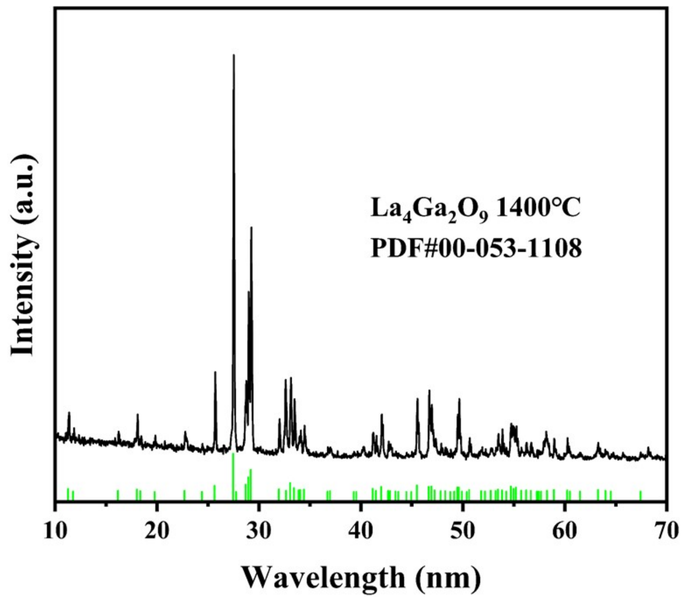

Figure S1. XRD patterns of $LaGaO_4$ powder samples.

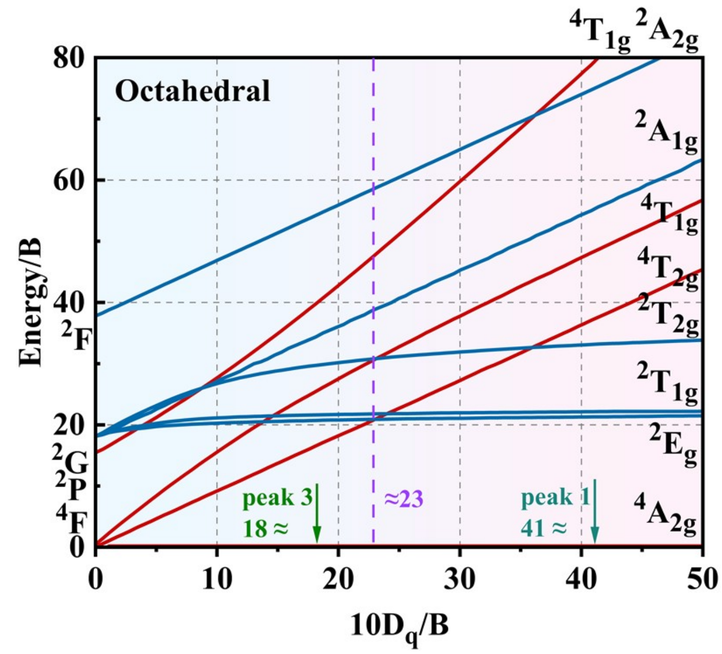

Figure S2. Tanabe-Sugano energy level diagram for Cr^{3+} ions ($^3d_3$) lying in the octahedral ligand.

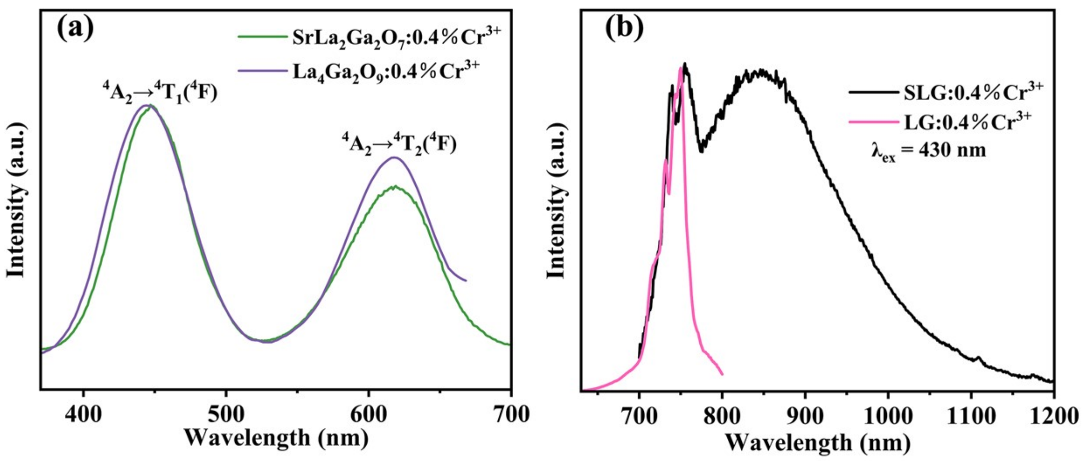

Figure S3. (a) PLE spectra recorded at RT, (b) PL spectra of SLG:0.4%Cr^{3+} and LG:0.4%Cr^{3+} phosphors.

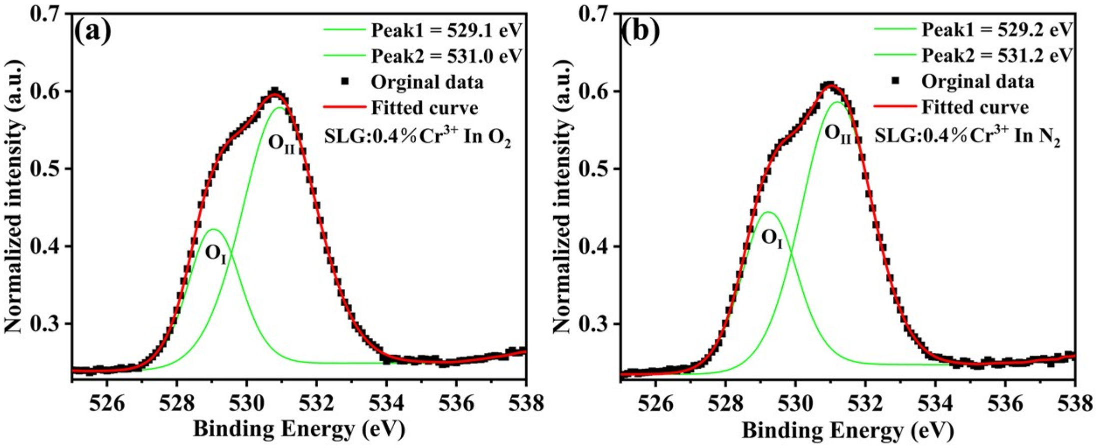

Figure S4. The XPS analysis of O 1s spectra for SLG:0.4%Cr^{3+} phosphors prepared (a) in O_2 atmosphere and (b) in N_2 atmosphere, with fitted peaks (O_I and O_{II}).

Table S1. Luminescence performance parameters of several Cr^{3+}-doped near-infrared fluorescent powders.

Hosts	λ_{ex}(nm)	λ_{em}(nm)	FWHM (nm)	IQE/EQE(%)	I_{423K}/I_{298K}(%)	Refs.
K_3AlF_6	430	750	100	\	\	1
$Gd_3Sc_2Ga_3O_{12}$	460	754	90	60	100	2
$Ba_2LaGa_{11}O_{20}$	468	738	133	\	34	3
$SrGa_2O_4$	420	780	170	\	56	4
$LiScSi_2O_6$	460	845	156	64.4/33.4	75	5
$SrLaMgTaO_6$	470	810	180	37.8/14.18	80.4	6
$Na_3Ga_2Li_3F_{12}$	430	764	117	48.7/7.79	71	7
Na_3ScF_6	436	774	108	91.5/40.82	\	8
Na_3AlF_6	420	720	95	75	60	9
K_3ScF_6	432	770	150	71.7	87.3	10
K_2NaScF_6	435	765	100	74	89.6	11
Sr_2MgWO_6	371	763	125	\	\	12
Ca_2MgWO_6	371	800	150	\	\	13
La_2MgZrO_6	460	825	210	58	50	14
$GdAl_3(BO_3)_4$	420	733	80	91	88	15
$La_3Sc_2Ga_3O_{12}$	490	800	145	35	60	16

$LiSrAlF_6$	436	820	155	52.06	55.47	17

Reference

1 C. Lee, Z. Bao, M. Fang, T.. Lesniewski, S. Mahlik, M. Grinberg, G. Leniec, S. M. Kaczmarek, M. G. Brik, Y. T. Tsai, T. L. Tsai and R. S. Liu, Chromium (III)-doped fluoride phosphors with broadband infrared emission for light-emitting diodes, *Inorg. Chem.*, 2019, **59**, 376-385.

2 B. Malysa, A. Meijerink and T. Jüstel, Temperature dependent Cr^{3+} photoluminescence in garnets of the type $X_3Sc_2Ga_3O_{12}$ (X= Lu, Y, Gd, La), *J. Lumin.*, 2018, **202**, 523-531.

3 L. Dong, J. Hou, B. Shao, S. Zhao and Y. Fang, $Cr^{3+}/Yb^{3+}/Nd^{3+}$-doped $Ba_2LaGa_{11}O_{20}$ broadband NIR phosphors for NIR pc-LED and c-Si solar cells, *Opt. Mater.*, 2022, **127**, 112290.

4 K. Sudarshan, A.Balhara, M.S. Kambli, R.T. Parayil, S.M. Patil and S.K. Gupta, Multiple local site Cr^{3+} emission leading to broadband NIR light in novel $SrGa_2O_4$ phosphors, *Mater. Res. Bull.*, 2024, **169**,1.1-1.9

5 Y. Yan, M. Shang, S. Huang, Y. Wang, Y. Sun, P. Dang and J. Lin, Photoluminescence Properties of $AScSi_2O_6$:Cr^{3+} (A=Na and Li)Phosphors with High Efficiency and Thermal Stability for Near-Infrared Phosphor-Converted Light-Emitting Diode Light Sources, *ACS Appl. Mater. Interfaces.*, 2022, **6**, 8179-8190.

6 Y. Fan, H. Wu, Y. Li and Y. Hu, Highly thermally stable $SrLaMgTaO_6$:Cr^{3+}

double-perovskite phosphors fornight-vision applications, *Ceram. Int.*, 2024, **50**, 28707-28714.

7 W. Nie, Y. Li, J. Zuo, Y. Kong, W. Zou, G. Chen, J. Peng, F. Du, L. Han and X. Ye, Cr^{3+}-Activated $Na_3X_2Li_3F_{12}$ (X = Al, Ga, or In) Garnet Phosphors with Broadband NIR Emission and High Luminescence Efficiency for Potential Biomedical Application, *Mater Chem C.*, 2021, **9**, 15230−15241.

8 F. He, E. Song, Y. Zhou, H. Ming, Z. Chen, J. Wu, P. Shao, X. Yang, Z. Xia and Q. Zhang, A general ammonium salt assisted synthesis strategy for Cr^{3+}-doped hexafluorides with highly efficient near infrared emissions, *Adv. Funct. Mater.*, 2021, **31**, 2103743.

9 D. Yu, Y. Zhou, C. Ma, J. H. Melman, K. M. Baroudi, M. LaCapra and R. E. Riman, Non-rare-earth Na_3AlF_6: Cr^{3+} phosphors for far-red light-emitting diodes, *ACS Appl. Electron. Mater.*, 2019, **1**, 2325-2333.

10 H. Yu, J. Chen, R. Mi, J. Yang and Y. Liu, Broadband near-infrared emission of K_3ScF_6: Cr^{3+} phosphors for night vision imaging system sources, *Chem. Eng. J.*, 2021, **417**, 129271.

11 E. Song, H. Ming, Y. Zhou, F. He, J. Wu, Z. Xia and Q. Zhang, Cr^{3+}-Doped Sc-based fluoride enabling highly efficient near infrared luminescence: a case study of K_2NaScF_6: Cr^{3+}, *Laser Photonics Rev.*, 2021, **15**, 2000410.

12 D. Xu, Z. Qiu, Q. Zhang, L. Huang, Y. Ye, L. Cao and J. Meng, Sr_2MgWO_6: Cr^{3+} phosphors with effective near-infrared fluorescence and long-lasting phosphorescence, *J. Alloys Compd.*, 2019, **781**, 473-478.

13 D. Xu, X. Wu, Q. Zhang, W. Li, T. Wang, L. Cao and J. Meng, Fluorescence property of novel near-infrared phosphor Ca_2MgWO_6: Cr^{3+}. *J. Alloys Compd.*, 2018, **731**, 156-161.

14 H. Zeng, T. Zhou, L. Wang and R. Xie, Two-site occupation for exploring ultra-broadband near-infrared phosphor double-perovskite La_2MgZrO_6: Cr^{3+}, *Chem. Mater.*, 2019, **31**, 5245-5253.

15 D. Huang, H. Zhu, Z. Deng, H. Yang, J. Hu, S. Liang, D. Chen, E. Ma and W. Guo, A highly efficient and thermally stable broadband Cr^{3+}-activated double borate phosphor for near-infrared light-emitting diodes, *J. Mater. Chem. C*, 2021, **9**, 164-172.

16 B. Malysa, A. Meijerink and T. Jüstel, Temperature dependent Cr^{3+} photoluminescence in garnets of the type $X_3Sc_2Ga_3O_{12}$ (X= Lu, Y, Gd, La), *J. Lumin.*, 2018, **202**, 523-531.

17 D. Wu, L. Liu, H. Liang, H. Duan, W. Nie, J. Wang, J. Peng and X. Ye, $LiBAlF_6$: Cr^{3+} (B= Ca, Sr) fluoride phosphors with ultra-broad near-infrared emission for NIR pc-LEDs, *Ceram. Int.*, 2022, **48**, 387-396.